



# Fast Detection of Chloramphenicol in Raw Milk Using a Hairpin Aptamer-templated Silver Nanoclusters

Hengchao Li<sup>1,2</sup>, Bin Hu<sup>1,2</sup>, Yuliang Cheng<sup>1,2</sup>, Hang Yu<sup>2,3</sup>, Yunfei Xie<sup>1,2</sup>,  
Weirong Yao<sup>2,3</sup>, Yahui Guo<sup>1\*</sup> and He Qian<sup>2</sup>

<sup>1</sup>State Key Laboratory of Food Science and Technology, Jiangnan University, Wuxi, China.

<sup>2</sup>National Center for Technology Innovation on Fast Biological Detection of Grain Quality and Safety, School of Food Science and Technology, Jiangnan University, Wuxi, China.

<sup>3</sup>Qingdao Special Food Research Institute, Qingdao, Shandong Province, 266109, China.

## Authors' contributions

This work was carried out in collaboration among all authors. Authors HL and YG designed the study, performed the statistical analysis, wrote the protocol and wrote the first draft of the manuscript. Authors YC, HY, YX and WY managed the analyses of the study. Authors BH and HQ managed the literature searches. All authors read and approved the final manuscript.

## Article Information

DOI: 10.9734/AJOCS/2021/v9i419077

### Editor(s):

(1) Dr. Sung Cheal Moon, Korea Institute of Materials Science (KIMS), Republic of Korea.

### Reviewers:

(1) Yuan-Tsung Chen, National Yunlin University of Science and Technology, Taiwan.

(2) Flavia C. Zacconi, Pontificia Universidad Católica de Chile, Chile.

Complete Peer review History: <http://www.sdiarticle4.com/review-history/66371>

Original Research Article

Received 03 January 2021

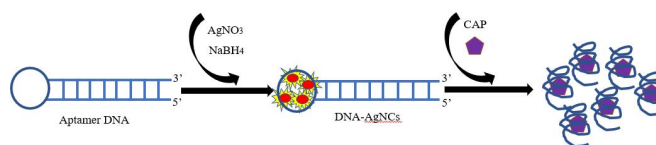
Accepted 10 March 2021

Published 07 April 2021

## ABSTRACT

In this presented work, a facile and efficient method was established for the detection of chloramphenicol (CAP) based on target-induced structure transformation of aptamer. This aptamer DNA with a hairpin structure can coincidentally serve as a template for the synthesis of bright silver nanoclusters (quantum yield 16.36%). The binding of CAP with aptamer DNA could cause the destruction of the hairpin structure, resulting in the quenching of the fluorescence of silver nanoclusters (AgNCs). It costs less than 10 minutes to complete the assay, and excellent sensitivity was achieved with detection limit of 0.052 nmol/L. The selectivity and recovery experiments also demonstrated satisfactory results of this proposed protocol. The method has potential applicability, and provides a new strategy for the development of label-free sensors based on aptamer and AgNCs.

\*Corresponding author: E-mail: guoyahui@jiangnan.edu.cn, 2630077187@qq.com;

**Graphical Abstract:**

**Keywords:** Chloramphenicol; silver nanoclusters; aptamer; fast detection.

## 1. INTRODUCTION

Antibiotics are widely used worldwide as antimicrobial drugs to treat diseases and promote animal growth. In recent years, food safety problems have been exposed continuously, and the current situation of food safety has become the focus of more and more people's attention. The overuse of antibiotics has become one of the biggest problems in the world. The abuse of antibiotics, which is an important reason of microbial antibiotic resistance [1,2], has led to many diseases, such as acute appendicitis, pediatric otitis media, and skin diseases, that are difficult to be cured. There is a case of antibiotics overuse in the adult urinary system that most of survey population had been treated with antibiotics and the anti-infection effect was not significantly improved [3-11]. The overuse of antibiotic treatment also has harmful effect on evolution and ecological environment. Most antibiotics ingested by humans and livestock are excreted into nature and thus increase the rate of mutation, recombination, etc., in all microbiome. For example, the overuse of antibiotics in the aquaculture industry is inevitable, and the associated antibiotic contamination and resistance pose an enormous threat to the ecosystem [12-15]. At the same time, a large number of antibiotics were injected into seawater, which greatly reduced the water quality of fishery resources and damaged the marine ecological environment. Therefore, it is very necessary and important to detect antibiotic residue in food. Now, many standard test methods such as high-performance liquid chromatography, gas chromatography-mass spectrometry, inductively coupled plasma mass spectrometry, liquid chromatography-mass spectrometry and chemiluminescence enzyme-linked immunosorbent [16-34] are accurate, the operations of those methods are cumbersome and expensive, Therefore, to develop simple, friendly economic, portable substitutes for determination of CAP is necessary [35-37].

Aptamers are double-stranded DNA or single-stranded RNA molecules that bind specific molecular targets [38]. Its function is similar to the antibody, and has many advantages, such as specificity, good affinity, simple synthesis method, good stability, easy modification, A wide range of target species, repeatable use. Therefore, the nucleic acid aptamer analysis was used in all kinds of tests, such as colorimetric analysis, chromatographic analysis, electrochemical sensors, biological imaging [39-42] and other areas of the application. Zhou et al. [43] developed a new type of unlabeled aptamer microfluidic electrophoresis (MCE) equipment for automatic detection of antibiotic residues, aptamer captured CAP and the whole system contained the partial complementary oligonucleotide of aptamer, which detected by MCE platform that can produce different fluorescence signals. This measure owned many benefits, such as MCE was a good equipment, the detection time was short and the process was easy. Chen et al. [44] established a new electrochemical aptamer sensor to detect different antibiotics synchronously, the nanoscale metal organic framework (NMOF), which was used to take multiple metal ions, was connected with Kanamycin and CAP's complementary DNA series of aptamers to obtain two signals. Square wave voltammetry can detect the NMOFs when antibiotics connected with aptamers. This method owned many merits, including the high sensitivity and excellent selectivity. However, all of these methods require labeling process, which were expensive and cumbersome.

Metal nanocluster (MNC) is an excellent fluorescent nanomaterial, which refer to the nanomaterials that can produce fluorescence by absorbing energy and releasing it in the form of radiation transition [45-49]. Compared with dyes and quantum dots, MNC including AuNCs, AgNCs, CuNCs, and PtNCs, which have been widely synthesized and characterized, has many advantages, for example small size, good dispersion, good photobleaching resistance, high

light absorption coefficient, and low cytotoxicity [50-57]. AgNCs is a kind of metal nanoclusters that have been widely studied. As a kind of precious metal, silver has similar properties to gold, and the price of silver is relatively cheap and easier to obtain. Compared with CuNCs, AgNCs has better stability. Moreover, conventional probes need to be functional modification and purified, which greatly increases the preparation time of materials and the cost of probe synthesis, nevertheless, the synthesis of AgNCs does not require covalent modification process.

As a kind of label-free signal reporter, DNA-templated silver nanoclusters (DNA-AgNCs) have gained great attention in the development of biosensors. The advantages of AgNCs include low cost, no chemical modification and link, easy realization of multi-signal output, simple synthesis method, strong photobleaching resistance, high fluorescence quantum yield, low toxicity and good biocompatibility [58-60]. The syntheses of AgNCs using DNAs as templates endow the DNA-AgNCs with inherent recognition function of DNA or aptamer. For instance, Shen et al. [61] proposed an unlabeled DNA detection method based on EXO-III assisted amplification and DNA hairpin -AgNCs with high quantum yield. Xu et al. [62] coupled DNA-AgNCs with target recirculation amplification assisted by nucleic acid exonuclease III, and designed a new unlabeled fluorescence detection method. Shen et al. [63] first obtained spring green luminescent AgNCs by using the "lightbulb" DNA structure as a synthesis template. This method had many advantages, for example, none of chemical modification, low cost of probe preparation, and high flexibility of method design.

In our work, we found that the CAP aptamer DNA with stem-loop structure can be synthesized AgNCs and the combination of CAP and its aptamer can influence the fluorescence intensity. After synthesis, the fluorescence signal of AgNCs was significantly enhanced. After the addition of CAP, the AgNCs was destroyed by the combination of CAP and its aptamer, and the fluorescence was significantly weakened. Based on these, a promising aptamer method for nucleic acid was developed and could be applied in raw milk.

## 2. MATERIALS AND METHODS

### 2.1 Reagents

All nucleic acid sequences displayed in Table S1 were synthesized by Sangon Biotechnology Co.,

Ltd (Shanghai, China). The stock solution of DNA/RNA was prepared in ultrapure water and accurately quantified based on the UV absorbance at a wavelength of 260 nm. The buffer solutions for all experiments were 1 × TAE, 1 × TBE, 1 × TE, 1 × PB, 1 × PBS. All other chemicals were purchased from Sinopharm Chemical Reagent Co., Ltd. (Shanghai, China), and used without further purification. The ultrapure water used was purified by a Milli-Q A10 filtration system (18.2 MU cm). All solutions were prepared using distilled water and stored at 4°C before use.

### 2.2 Reaction

The concentration of CAP aptamer was accurately quantified by measuring the absorbance at 260 nm, and the DNA-AgNCs was synthesized. The total reaction system was 200 uL, including 10 uL of CAP aptamer, 165 uL of ultrapure water, 20 uL of buffer solution, 3 uL of silver nitrate and 2 uL of sodium borohydride. The fluorescence was measured after 9 hours of reaction at room temperature [64-66].

### 2.3 Detection of CAP

In the sensor detection, the pre-configured CAP solution was added into the above reaction system and the concentration of CAP in the final system was 0 nmol/L, 0.5 nmol/L, 1 nmol/L, 2 nmol/L, 4 nmol/L, 8 nmol/L, 10 nmol/L, 12 nmol/L, 14 nmol/L, 18 nmol/L, 20 nmol/L, 40 nmol/L, 80 nmol/L, 100 nmol/L. The total system was fully shaken for 1 minute to make it evenly mixed and placed in a dark place at room temperature. Using the above testing steps, the antibiotics, which reacted with DNA-AgNCs, were changed from CAP to kanamycin, gamithromycin, bleomycin, streptomycin, oxytetracycline, and penicillin respectively. The results were compared with those of CAP results to evaluate the selectivity of the probe. CAP or other antibiotics with a final concentration of 10 nmol/L were used in both optimization and selectivity experiments. In addition, the sequence with similar CAP aptamer was used to determine whether CAP reacted with its aptamer to reduce the fluorescence intensity. The fluorescence was measured after 0.5 hour.

### 2.4 Detection of CAP in Milk

First, 4.0 mL raw milk was put into a 15 mL centrifuge tube, diluted to 10 mL, and 10% trichloroacetic acid and chloroform mixed

solution was added to 2.0 mL, and the protein was vortex stirred for 1 min to precipitate in the sample matrix. The mixture was ultrasound treated at 20 °C for 15 minutes and centrifuged at 5000 rpm for 10 minutes to separate the sediment. Secondly, the supernatant was transferred to another centrifuge tube. After centrifugation at 5000 rpm for 10 minutes, precipitation was removed again and detected with the final solution.

## 2.5 Measurements

The absorption of DNA-AgNCs solution at 260 nm was recorded on Eppendorf Ag 22331 Humburg (Germany). All fluorescence measurements were performed on a fluorescence spectrophotometer (f-4600, Hitachi, Japan). The xenon lamp was used as the excitation source, and a quartz fluorescent cup with an optical path length of 1.0 cm was used. The fluorescence intensity was measured at room temperature. According to the repeated quantification, the excitation wavelength was set at 442 nm and the recording emission range was 470-600 nm. The excitation and emission bandwidth were set at 10 nm, and the maximum fluorescence emission spectrum was 520 nm. Before each measurement, clean the reaction cup with 70% ethanol and ultrapure water for three times.

## 3. RESULTS AND DISCUSSION

### 3.1 Principle

The enormous DNA templates of different sequences and structures, such as single-stranded DNA (ssDNA), double-stranded DNA

(dsDNA), triplex DNA, DNA hairpin etc., were used to synthesize versatile DNA-AgNCs. Among the templates, what the most used template was DNA hairpin because of its simple secondary structure yet efficient encapsulation of AgNCs. For instance, Oneill P R et al. [67] studied the relationship between the structure of hairpin AgNCs and fluorescence signal by using the ring containing 3-12 cytosines (C). The results showed that almost all C-ring hairpins had obvious fluorescence peaks, and their wavelength and intensity varied with the number of C-bases in the ring. Gwinn et al. [68] studied the DNA hairpin structures containing different base pairs of stems and rings. They studied four kinds of base (C/T/G/A) hairpins, and the results showed that the C-loop hairpins had the highest fluorescence intensity. In our design, as shown in Fig. 1, in the absence of CAP, DNA has a loop circular structure. AgNCs are introduced to form DNA-AgNCs at the circular structure to increase the fluorescence signal. When CAP was introduced, CAP combined with its aptamer, which destroyed the structure of DNA-AgNCs and reduced the fluorescence intensity. The initial system consisted of 100 nmol/L CAP aptamer sequence, 3 mmol/L silver nitrate and 3 mmol/L sodium borohydride. As shown in picture, it was found to be stable (maximum fluorescence intensity state) in the absence of CAP (black line). However, when CAP (2 uL) was added to the system, the fluorescence intensity decreased significantly (red line). The addition of 10 nmol/L CAP can quench about half of the maximum fluorescence and the reaction efficiency is very high. Therefore, it is the introduction of CAP that leads to the decrease of fluorescence signal.

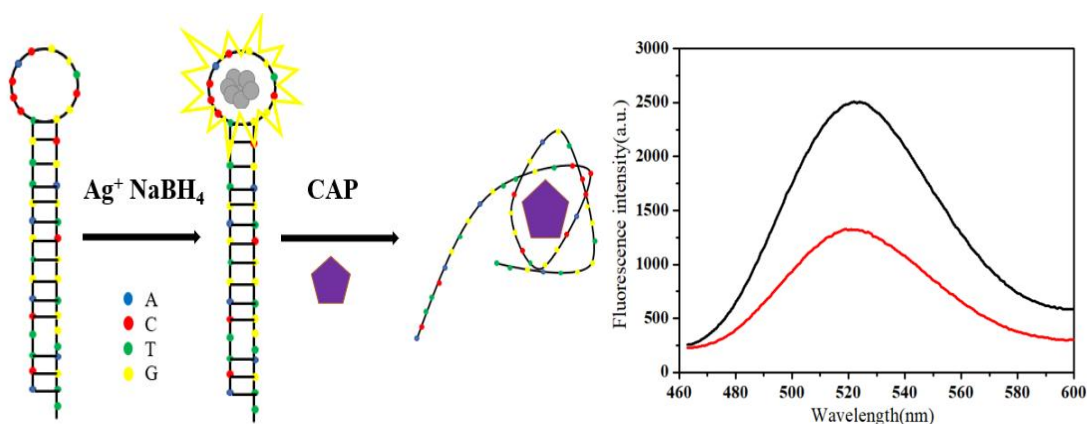


**Fig. 1. Schematic diagram of nucleic acid sensor detecting CAP. Feasibility of the system. The fluorescence emission spectra of 0 nmol/L CAP (black line), 10 nmol/L CAP (red line)**

In order to further verify the feasibility of the method, a series of control experiments are carried out, and the results are shown in Fig. S1 (a) of SI. First, C<sub>6</sub>G<sub>5</sub>C<sub>6</sub> (probe sequence) was used to see whether it was a non-specific quenching mechanism or not, and it was found that there was indeed a little quenching. Then the aptamer was modified and still able to synthesize AgNCs, but perhaps unable to interact with CAP because the signal was found to decrease slightly. Therefore, it shows that the quenching mechanism has both aptamer-specific and non-specific characteristics.

Quantum dots or carbon dots detect CAP based on the electron absorption quenching of CAP. With CAP as the target molecule, carbon spot (CDs) as the fluorescence detection probe, and molecularly imprinted polymer (MIP) as the selective enrichment container, Chen et al. [69] designed a molecularly imprinted fluorescence sensor based on carbon point, which can be used for the specific detection of CAP in food system. Li et al. [70] established a fluorescence detection sensor based on the fluorescence quenching of soybean protein gold nanoclusters (SP-AuNCs) by CAP. These methods are not selective for similar substances because they are based on positive and negative electron interactions or rich electron group-electron absorption group interactions. To verify the principle of our scheme again, we synthesized AgNCs using two non-aptamer DNA templates and detected CAP. The results were shown in Fig. S1 (b,c) of SI that the fluorescence intensity was significantly reduced only when the original CAP aptamer sequence was added, indicating that the target sequence was easy to react with CAP, leading to the dissolution of a large number of DNA-AgNCs. However, the other sequences could not react with CAP, and the fluorescence intensity did not change significantly, indicating that the modified base sequences destroyed the original configuration of CAP binding. DNA can form some special secondary structures that serve as templates for the synthesis of AgNCs, the fluorescence properties of AgNCs are closely related to the secondary structure of DNA [71-79]. Gwinn et al. [68] studied the difference between single-stranded DNA and hairpin DNA used to synthesize AgNCs, and found that the Hairpin structure synthesis with C ring AgNCs have the greatest fluorescence intensity. Li et al. [80] found that the base pairs in double chain, other than the ring area, also helps the formation of AgNCs. As seen from Fig. S1 of SI, the modified

CAP aptamer could not bind to CAP, resulting in an insignificant decrease in fluorescence. Therefore, the DNA-AgNCs structure was not changed at this time. However, the unmodified CAP aptamer can combine with CAP and its fluorescence decreases significantly. At this time, the combination of CAP and its aptamer leads to the change of the original structure and the release of a large amount of Ag<sup>+</sup>, because the existence of the ring has the role of protecting AgNCs [80]. The results showed that the conformation of CAP aptamer was changed after the reaction.

### 3.2 Optimization of Experimental Conditions

For the whole aptamer reaction, the main influencing factors include buffer, pH, the concentration ratio of silver nitrate to DNA, reaction temperature and reaction time.

Different concentrations of silver nitrate can lead to different fluorescence signals, for example, a low concentration may lead to low fluorescence signal after synthesis, while a high concentration may lead to the decrease of fluorescence intensity due to metal ion quenching. Therefore, it is very important to optimize the concentration ratio, which is the key to ensure aptamer reaction. When different amounts of silver nitrate solution were added, the fluorescence intensity was measured after the reaction was fully carried out at room temperature. As shown in Fig. 2(a), the fluorescence intensity increased with the concentration ratio of silver nitrate to DNA. However, when the ratio of silver nitrate to DNA reached 9:1, the fluorescence intensity reached the maximum, that is, the reaction reached the maximum fluorescence intensity. Therefore, the ratio of silver nitrate to DNA was 9:1 to start the following reaction.

Different reaction time can produce different fluorescent signals. A long or a short reaction time can affect the experiment. Therefore, optimization of reaction time is also a key factor. As we can be seen from the Fig. 2(b), after adding different concentrations of CAP solutions to the DNA-AgNCs system, a rapid reaction occurred immediately. The reaction in the 600 seconds tended to be stable. Therefore, the optimal response time under this system is 10 minutes. Therefore, we can obtain the rapid detection time of CAP.

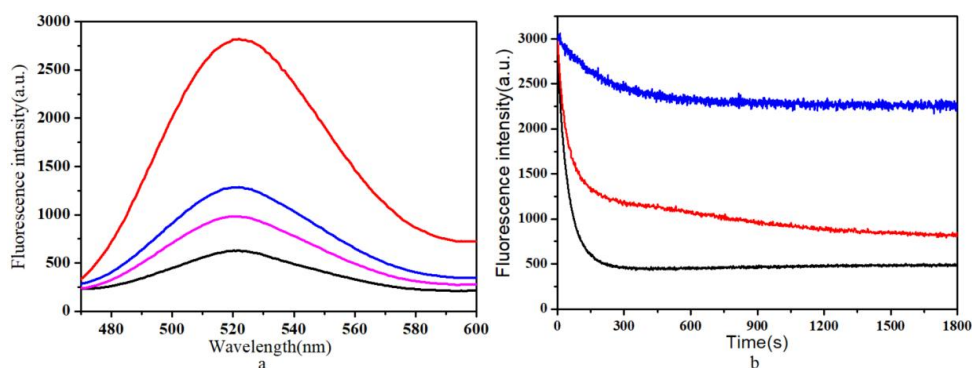


**Fig. 2. Optimization of experimental conditions. (a) Evaluation of the effect of the concentration ratio of silver nitrate to DNA (The ratios of black, pink, red and blue line are 3:1, 6:1, 9:1 and 12:1 respectively). (b) Optimization of time (The CAP concentrations of blue, red and black line are 1 nmol/L, 20 nmol/L and 100 nmol/L respectively)**

In order to improve the detection sensitivity and experimental efficiency, the buffer and pH are optimized because different buffer and pH can lead to different fluorescence signals. To study the effect of buffer and pH (Fig. 3), the method is to synthesize DNA-AgNCs with different buffer and pH, record the fluorescence signal intensity, and then add CAP to detect the fluorescence signal intensity again. The fluorescence intensity of the synthesized DNA-AgNCs was affected by different buffers and pH values, optimization of DNA-AgNCs synthesis conditions is beneficial to improve the detection output signal. As seen from Fig. 3, the synthetic fluorescence intensity of DNA-AgNCs using PBS buffer was higher than that of other buffers. Therefore, the fluorescence intensity may be caused by DNA - AgNCs synthesis conditions. The most likely reason is that the influence of the buffer, TE, TBE and TAE contain a lot of  $\text{Cl}^-$ , which affects the synthesis of DNA-AgNCs, because too much  $\text{Cl}^-$  combine

with  $\text{Ag}^+$  to form  $\text{AgCl}_2$  [81]. Under alkaline or acidic conditions, the fluorescence properties of DNA-AgNCs are easily affected [82]. For one thing, under low pH conditions, the protonation of DNA bases weakens the interaction between C base and  $\text{Ag}^+$ , which is not conducive to the formation of DNA-AgNCs. For another, under the condition of high pH conditions, the concentration of  $\text{Ag}^+$  may be reduced due to the interaction between  $\text{Ag}^+$  and the phosphate group on DNA, and the interaction between C- $\text{Ag}^+$ -C is weakened, which is not conducive to the formation of DNA-AgNCs, thus leading to the decrease of fluorescence intensity of DNA-AgNCs [83-85]. The results showed that the optimum reaction condition was PBS (1) pH 6.5 at room temperature. In conclusion, the optimal operating conditions for this test: PBS (1) buffer with pH6.5, the concentration ratio of  $\text{AgNO}_3$  / DNA is 9:1, and the reaction time can be shortened to 10 minutes.

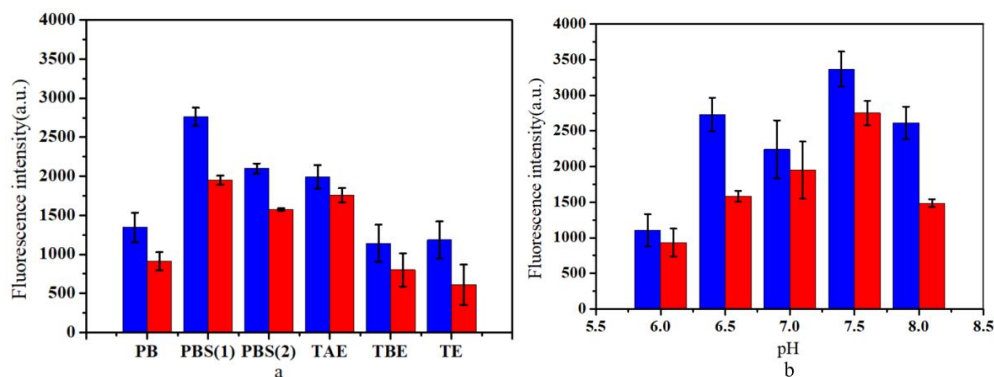


**Fig. 3. Optimization of experimental conditions. (a) Evaluation of the effect of the different buffer solutions. (b) The evaluation effect of pH**

### 3.3 Sensitivity and Specificity Investigation for the Assay

The relative fluorescence intensity ( $IF = (F_0 - F) / F_0$ ) was regarded as a coordinate to represent the optimization result, where  $F$  and  $F_0$  represent the fluorescence intensity in the presence and absence of CAP respectively. Under the optimized conditions, CAP with different concentrations from 0.5 to 100 nmol/L was detected. As shown in Fig. 4(a), with the increase of CAP concentration, the fluorescence intensity of the reaction system decreased significantly. This indicates that the AgNCs is destroyed gradually with the increase of CAP concentration and the combination of CAP and its aptamer. In addition, as shown in Fig. 4(b), the fluorescence changes showed a significant linear correlation ( $R^2 = 0.997$ ). The regression equation is  $y = 0.02867x + 0.15709$ , and the detection limit (LOD) is 0.052 nmol/L ( $3S / K$ ,  $S$  is the standard deviation of blank sample, and  $K$  is the slope of linear calibration curve), which means that about 52 pmol/L of CAP can be detected in 1 mL detection system. Compared with the existing aptamer detection methods, this method has similar detection limit, simple reaction process and simple sequence design. In fact, this method needs further improvement, especially compared

with the electrochemical nucleic acid sensor, the electrochemical nucleic acid sensor has lower background signal, more sensitive and better stability. Therefore, this method has a good application prospect on electrochemical platform.

In addition, the target DNA and different antibiotics (Gamithromycin, Oxytetracycline, Penicillin, Bleomycin, Kanamycin, Streptomycin) were detected with the same selectivity (Fig. 5). The results showed that the target DNA and CAP have specific binding capacity, because only CAP can cause the change of target DNA conformation, while any other antibiotics could not bind to the target DNA. Therefore, the method showed acceptable performance in the detection of antibiotic specificity.

In order to verify the accuracy and reliability of this method, the recovery tests of CAP with different concentrations (1 nmol/L, 10 nmol/L, 20 nmol/L) were carried out. Considering the practicability of this method in complex samples, milk was selected as substrate. As shown in Table 1, the recovery rate of CAP in milk was between 84.01% and 102.90%, indicating that the method has good accuracy and can be used for the detection of actual samples.

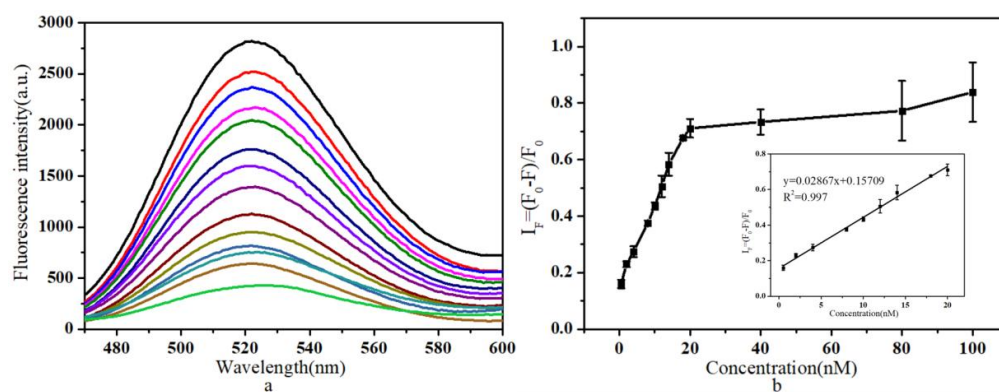


**Fig. 4. Sensitivity of the reaction. (a) Fluorescence emission spectra (0.5-100 nmol/L). (b) Relative fluorescence intensity (IF) corresponding to different concentrations of target DNA. Inset: linear range between IF and target concentration (0.5-20 nmol/L)**

**Table 1. Recovery analysis of target DNA**

Group	Additive amount (nmol/L)	Recovery rate (%)	RSD (n=3) (%)
Control	0	-	-
Label a	1	84.01	5.34
Label b	10	101.15	1.72
Label c	20	102.90	5.38

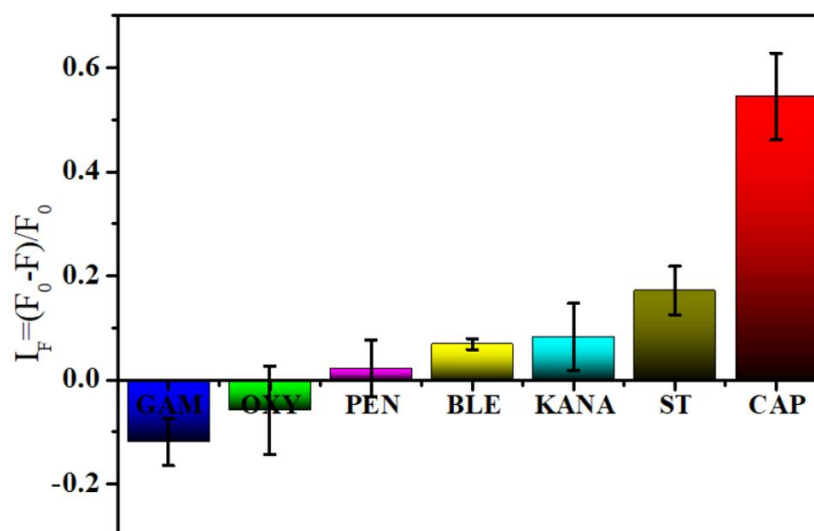


**Fig. 5. Selectivity assessment of the proposed method. Selectivity toward different antibiotics (The concentrations of different antibiotics are 10 nmol/L)**

#### 4. CONCLUSION AND FUTURE PERSPECTIVES

In conclusion, a novel fluorescent sensor based on aptamer was established to detect antibiotics. The strategy is based on the employment of CAP aptamer sequence for the synthesis of DNA-AgNCs. After adding CAP, a series of reactions are carried out to realize specific detection. The method does not contain any enzymes. The aptamer sequence is simple, accessible, and can be detected conveniently at room temperature. The detection limit is 0.052 nmol/L, which is low enough to meet China National Standard 0.1 ug/kg. The standard material for quantum yield measurement was rhodamine 6G, and the quantum yield was 16.36%. Moreover, compared with other CAP aptamer detection methods, the stability of this method still needs to be improved. Due to excellent fluorescent properties, DNA - AgNCs can be used as a fluorescence molecular probe to build biological sensors used in food analysis and detection, including bacterial, virus, heavy metal, biological toxins, Farmers additives, and illegal veterinary drug residue. Zhang et al. [86] used salmonella aptamer sequences and hairpin DNA template sequences, combining chain displacement amplification, to design a label-free fluorescence detection method for salmonella. Chen et al. [87] developed a detection of fluorescence signal biosensor based on DNA-AgNCs, using ochratoxin A aptamer and magnetic bead structure transformation of ochratoxin A. Chen et al. [88] proposed to

combine the malathion aptamer with the C rich sequence used for the synthesis of AgNCs as a probe, when malathion bind to aptamer, the space conformation probe changed and the color of solution turned brown, which can be used in detection of malathion. Dong et al. [89] used oligonucleotides with two structural domains, one of them can form AgNCs, another was aptamer having affinity for cocaine. In the absence of cocaine, the fluorescence of AgNCs was low, while in the presence of cocaine, the fluorescence was high. At present, the most important application of our design is detecting CAP. Based on the above designs, our plan will combine more strategies, having a wider range of application in the future. It is expected to achieve better results when combined with other strategies, such as electrochemical adapter sensor [90,91], colorimetric aptamer sensor [92-99], strand displacement amplification reaction (SDA) [100-102], hybridization chain reaction (HCR) [103-106] and catalyzed hairpin assembly (CHA) [107-109]. In addition, through the recovery test in milk, the practicability was verified successfully. The experimental results show that this method provides valuable information for the study of aptamer fluorescent sensor for the detection of antibiotics.

#### DISCLAIMER

The products used for this research are commonly and predominantly use products in our area of research and country. There is absolutely



no conflict of interest between the authors and producers of the products because we do not intend to use these products as an avenue for any litigation but for the advancement of knowledge. Also, the research was not funded by the producing company rather it was funded by personal efforts of the authors.

## CONSENT

Informed consent was obtained from all individual participants included in the study.

## COMPETING INTERESTS

Authors have declared that no competing interests exist.

## REFERENCES

1. Koliopoulos P, Kayange N M, Daniel T, et al. Multiplex-RT-PCR-ELISA panel for detecting mosquito-borne pathogens: *Plasmodium sp.* preserved and eluted from dried blood spots on sample cards [J]. *Malaria Journal*. 2021;20(1).
2. Gillings, Michael R. Evolutionary consequences of antibiotic use for the resistome, mobilome and microbial pangenome [J]. *Frontiers in Microbiology*. 2013;4(4):4.
3. Brown CA. Reducing outpatient antibiotic prescribing for acute respiratory infections: A quasi-experimental study [J]. *Journal of Doctoral Nursing Practice*. 2018;11(1):3-15.
4. Surlemont J, Lecuelle D, Courbier G, et al. Antibiotic therapy in pediatric acute appendicitis: Compliance with local protocol to reduce antibiotic overuse[J]. *Archives de Pédiatrie*; 2020.
5. Chon SY, Doan HQ, Mays RM, et al. Antibiotic overuse and resistance in dermatology [J]. *Dermatologic Therapy*. 2012;25(1):55-69.
6. Bassetti M, Melica G, Cenderello G, et al. Gram-positive bacterial resistance. A challenge for the next millennium [J]. *Panminerva Medica*. 2002;44(3):179.
7. Ameline A, Taquet MC, Terrade JE, et al. Identification of chloramphenicol in human hair leading to a diagnosis of factitious disorder [J]. *Clinical Toxicology*. 2020; 58(2):1-5.
8. Immunization with a biofilm-disrupting nontypeable haemophilus influenzae vaccine antigen did not alter the gut microbiome in chinchillas, Unlike oral delivery of a broad-spectrum antibiotic commonly used for otitis media [J]. *American Society for Microbiology*. 2020;5: e00296-20.
9. Mordi RM, Momoh MI. A five year study on the susceptibility of isolates from various parts of the body [J]. *African Journal of Biotechnology*. 2008;7(19):3401-3409.
10. Gill JM, Fleischut P, Haas S, et al. Use of antibiotics for adult upper respiratory infections in outpatient settings: A national ambulatory network study [J]. *Family Medicine*. 2006;38(5):349-54.
11. Arason VA, Sigurdsson JA. The problems of antibiotic overuse [J]. *Scandinavian Journal of Primary Health Care*. 2010; 28(2):65.
12. Ming Zhang A, et al. "Effectively reducing antibiotic contamination and resistance in fishery by efficient gastrointestinal-blood delivering dietary millispheres." *Journal of Hazardous Materials*; 2020.
13. Zhang H, Wang J, Zhou B, et al. Enhanced adsorption of oxytetracycline to weathered microplastic polystyrene: Kinetics, isotherms and influencing factors [J]. *Environmental Pollution*. 2018;243(P.T.B): 1550-1557.
14. Imran M, Das KR, Naik MM. Co-selection of multi-antibiotic resistance in bacterial pathogens in metal and microplastic contaminated environments: An emerging health threat [J]. *Chemosphere*. 2019; 215:846-857.
15. Yu F, Li Y, Huang G, et al. Adsorption behavior of the antibiotic levofloxacin on microplastics in the presence of different heavy metals in an aqueous solution [J]. *Chemosphere*. 2020;260:127650.
16. Kikuchi H, Sakai T, Teshima R, et al. Total determination of chloramphenicol residues in foods by liquid chromatography-tandem mass spectrometry [J]. *Food Chemistry*. 2017;230:589-593.
17. Po-Hsun Lin, Shih-Lun Yen, Ming-Shen Lin, et al. Microcalorimetric studies of the thermodynamics and binding mechanism between l-tyrosinamide and aptamer [J]. *The Journal of Physical Chemistry B*. 2008;112(21):6665-73.
18. Yangbao Miao, Gan N, Li T, et al. A colorimetric aptasensor for chloramphenicol in fish based on double-stranded DNA antibody labeled enzyme-linked polymer nanotracers for signal amplification [J]. *Sensors and Actuators B: Chemical*. 2015;220:679-687.

19. Xia W. Development of methods for detection of antibiotics residues in milk [J]. Food & Fermentation Industries. 2004; 30(7):112-116.
20. Lidija Kozačinski, Andrea Benussi Skukan, Ivana Filipović. Methods for detection of antibiotics and sulphonamides in meat [J]. Meso. 2006;viii(1):37-42.
21. Kim EA, Kwak HS. Comparison of methods for detection of antibiotics in milk [J]. Korean Journal of Dairy science; 1991.
22. Bedenic B, Vranes J, Mihaljevic LJ, et al. Sensitivity and specificity of various beta-lactam antibiotics and phenotypical methods for detection of TEM, SHV and CTX-M extended-spectrum beta-lactamases [J]. Journal of Chemotherapy. 2007;19(2):127-139.
23. YANO, Nobuhiro, ISHII, et al. Modification of the disk assay method for detection of antibiotics by direct seeding of spores of bacillus stearothermophilus [J]. Food Hygiene and Safety Science; 1975.
24. Babington R, Matas S, Marco MP, et al. Current bioanalytical methods for detection of penicillins [J]. Analytical and Bioanalytical Chemistry. 2012;403(6): 1549-1566.
25. Joshua Daniel Arias. Naturally-derived antibiotics from streptomyces zaomyceticus inhibit MRSA [J]; 2015.
26. Wang J, Hu Z, Feng L, et al. Determination of 22 antibiotics in disinfection products by ultra-performance liquid chromatography tandem mass spectrometry [J]. Journal of Hygiene Research. 2019;48(1):129-135.
27. Na W, Zhi-Li P, Jing-Yun F, et al. Determination of metabolites of nitrofurant antibiotics in pre-export pork by high performance liquid chromatography-tandem mass spectrometry [J]. Food science; 2008.
28. Ohmori T, Suzuki A, Niwa T, et al. Simultaneous determination of eight  $\beta$ -lactam antibiotics in human serum by liquid chromatography–tandem mass spectrometry [J]. Journal of Chromatography B. 2011;879(15-16):1038-1042.
29. Li N, Zhang X, Wu W, et al. Occurrence, seasonal variation and risk assessment of antibiotics in the reservoirs in North China [J]. Chemosphere. 2014;111:327-335.
30. Preinerstorfer B, Schiesel S, L Mmerhofer M, et al. Metabolic profiling of intracellular metabolites in fermentation broths from beta-lactam antibiotics production by liquid chromatography-tandem mass spectrometry methods [J]. Journal of Chromatography A. 2010;1217(3):312-328.
31. Melnik, Neumann AC, et al. Cloning and plant-based production of antibody MC10E7 for a lateral flow immunoassay to detect [4-arginine] microcystin in freshwater [J]. Plant Biotechnol J; 2018.
32. Ball HJ, Finlay D, Burns L, Mackie DP. Application of monoclonal antibody-based sandwich ELISAs to detect verotoxins in cattle faeces [J]. Research in Veterinary Science; 1994.
33. Panat A, Runglawan C, Prasert S, et al. Immunodiagnosis of fasciola gigantica infection using monoclonal antibody-based sandwich ELISA and immunochromatographic assay for detection of circulating cathepsin L1 protease [J]. Plos One. 2016;11(1): e0145650.
34. Chenard G, Bloemraad M, Kramps JA, et al. Validation of a monoclonal antibody-based ELISA to detect antibodies directed against swine vesicular disease virus [J]. Journal of Virological Methods. 1998;75(1): 105-112.
35. Scognamiglio V, Pezzotti G, Pezzotti I, et al. Biosensors for effective environmental and agrifood protection and commercialization: From research to market [J]. Microchimica Acta. 2010;170(3-4):215-225.
36. Verdian-Doghaei, A, Housaindokht MR. Spectroscopic study of the interaction of insulin and its aptamer – sensitive optical detection of insulin [J]. Journal of Luminescence. 2015;159:1-8.
37. Verdian-Doghaei A, Housaindokht MR, Bozorgmehr MR, et al. Conformational switch of insulin-binding aptamer into G-quadruplex induced by K<sup>+</sup> and Na<sup>+</sup>: An experimental and theoretical approach [J]. Journal of Biomolecular Structure and Dynamics. 2015;33(6):1153-1163.
38. Bock LC, Griffin LC, Latham JA, et al. Selection of single-stranded DNA molecules that bind and inhibit humanthrombin [J]. Nature. 1992; 355(6360):564-6.
39. Liu J, Lu Y. Preparation of aptamer-linked gold nanoparticle purple aggregates for colorimetric sensing of analytes [J]. Nature Protocols. 2006;1(1):246-252.
40. Deng Q, German I, Buchanan D, et al. Retention and separation of adenosine and analogues by affinity chromatography with

- an aptamer stationary phase [J]. *Analytical Chemistry*. 2001;73(22):5415-5421.
41. Hansen JA, Wang J, Kawde AN, et al. Quantum-dot/aptamer-based ultrasensitive multi-analyte electrochemical biosensor [J]. *Journal of the American Chemical Society*. 2006;128(7):2228-2229.
  42. Bagalkot V, Zhang L, Levy-Nissenbaum E, et al. Quantum dot-aptamer conjugates for synchronous cancer imaging, therapy and sensing of drug delivery based on bi-fluorescence resonance energy transfer [J]. *Nano Letters*. 2007;7(10):3065-3070.
  43. Zhou L, Gan N, Zhou Y, et al. A label-free and universal platform for antibiotics detection based on microchip electrophoresis using aptamer probes [J]. *Talanta*. 2017;167(Complete):544-549.
  44. Chen M, Gan N, Zhou Y, et al. A novel aptamer-metal ions- nanoscale MOF based electrochemical biocodes for multiple antibiotics detection and signal amplification [J]. *Sensors and Actuators, B: Chemical*. 2017;242:1201-1209.
  45. Lin CA, Yang TY, Lee CH, et al. Synthesis, characterization and bioconjugation of fluorescent gold nanoclusters toward biological labeling applications [J]. *Acs Nano*. 2009;3(2):395-401.
  46. Feng L, Huang Z, Ren J, et al. Toward site-specific, homogeneous and highly stable fluorescent silver nanoclusters fabrication on triplex DNA scaffolds [J]. *Nucleic Acids Research*; 2012;40(16): e122.
  47. Wang R, Lu KQ, Tang ZR, et al. Recent progress in carbon quantum dots: Synthesis, properties and applications in photocatalysis [J]. *Journal of Materials Chemistry A*. 2017;5(8):3717-3734.
  48. Martinez JS, Xie J. Preface for special topic: Few-atom metal nanoclusters and their biological applications [J]. *APL Materials*. 2017;5(5):053001.
  49. Jin RC. Atomically precise metal nanoclusters: Stable sizes and optical properties [J]. *Nanoscale*. 2015;7(5):1549-1565.
  50. Selvaprakash K, Chen YC. Using protein-encapsulated gold nanoclusters as photoluminescent sensing probes for biomolecules [J]. *Biosensors and Bioelectronics*. 2014;61:88-94.
  51. Lu YZ, Wei WT, Chen W. Copper nanoclusters: Synthesis, characterization and properties [J]. *Chinese Science Bulletin*. 2012;57(1):41-47.
  52. Xu HX, Suslick KS. Water-soluble fluorescent silver nanoclusters [J]. *Advanced Materials*. 2010;22(10):1078-1082.
  53. Kang X, Zhou M, Wang S, et al. The tetrahedral structure and luminescence properties of Bi-metallic Pt1Ag28(SR)18(PPh3)4 nanocluster [J]. *Chemical Science*. 2017;8(4):2581-2587.
  54. Ayesha AI, Thaker S, Qamhieh N, et al. Size-controlled Pd nanocluster grown by plasma gas-condensation method [J]. *Journal of Nanoparticle Research*. 2011;13(3):1125-1131.
  55. Aiken JD, Lin Y, Finke RG. A perspective on nanocluster catalysis: Polyoxoanion and (n-C4H9)4N+ stabilized Ir(0)~300 nanocluster 'soluble heterogeneous catalysts' [J]. *Journal of Molecular Catalysis A: Chemical*. 1996;114(24):29-52.
  56. Jin R. Atomically precise metal nanoclusters: Stable sizes and optical properties [J]. *Nanoscale*. 2015;7(5):1549-1565.
  57. Xavier PL, Chaudhari K, Baksi A, et al. Protein-protected luminescent noble metal quantum clusters: An emerging trend in atomic cluster nanoscience [J]. *Nano Reviews*. 2012; 3(1):14767-14782.
  58. Shang L, Dong S, Nienhaus GU. Ultra-small fluorescent metal nanoclusters: Synthesis and biological applications [J]. *Nano Today*. 2011;6(4):401-418.
  59. Zhang L, Wang E. Metal nanoclusters: New fluorescent probes for sensors and bioimaging [J]. *Nano Today*. 2014;9(1):132-157.
  60. Wilcoxon JP, Abrams BL. Synthesis, structure and properties of metal nanoclusters [J]. *Chemical Society Reviews*. 2006;35(11):1162-1194.
  61. Shen F, Cheng Y, Xie Y, et al. DNA-silver nanocluster probe for norovirus RNA detection based on changes in secondary structure of nucleic acids [J]. *Analytical Biochemistry*. 2019;583:113365.
  62. Xu M, Gao Z, Wei Q, et al. Label-free hairpin DNA-scaffolded silver nanoclusters for fluorescent detection of Hg2+ using exonuclease III-assisted target recycling amplification [J]. *Biosensors and Bioelectronics*. 2016;79:411-415.

63. Guo Y, Shen F, Cheng Y, et al. The light-up fluorescence of AgNCs in a "DNA bulb" [J]. *Nanoscale*. 2018;10.
64. Driehorst T, Oneill PR, Goodwin PM, et al. Distinct conformations of DNA-stabilized fluorescent silver nanoclusters revealed by electrophoretic mobility and diffusivity measurements [J]. *Langmuir*. 2011;27(14): 8923-8933.
65. Sengupta B, Ritchie CM, Buckman JG, et al. Base-directed formation of fluorescent silver clusters [J]. *Journal of Physical Chemistry C*. 2008;112(48):18776-18782.
66. Ritchie CM, Johnsen KR, Kiser JR, et al. Ag nanocluster formation using a cytosine oligonucleotide template [J]. *Journal of Physical Chemistry C*. 2007;111(1):175-181.
67. Oneill PR, Velazquez LR, Dunn DG, et al. Hairpins with poly-C loops stabilize four types of fluorescent AgNCs:DNA [J]. *Journal of Physical Chemistry C*. 2009; 113(11):4229-4233.
68. Gwinn E, Oneill PR, Guerrero A, et al. Sequence-dependent fluorescence of DNA-hosted silver nanoclusters[J]. *Advanced Materials*. 2010;20(2):279-283.
69. Chen S, Xie Y, et al. Molecular imprinted polymers based on carbon points were used to detect chloramphenicol in crucian carp [J]; 2019.
70. Chen Y, Li H, et al. Fluorescent gold nanoclusters were used for rapid detection of chloramphenicol in pork [J]. *Journal of Anhui Agricultural Sciences*. 2020;48: 644(07):221-226.
71. Petty JT, Zheng J, Hud NV, et al. DNA-templated Ag nanocluster formation [J]. *Journal of the American Chemical Society*. 2004;126(16):5207-5212.
72. Teng Y, Yang X, Han L, et al. The relationship between DNA sequences and oligonucleotide-templated silver nanoclusters and their fluorescence properties [J]. *Chemistry-A European Journal*. 2014;20(4):1111-1115.
73. Ma JL, Yin BC, Ye BC. DNA template-regulated intergrowth of a fluorescent silver nanocluster emitter pair [J]. *RSC Advances*. 2015;5(119):98467-98471.
74. Zhou W, Zhu J, Fan D, et al. A multicolor chameleon DNA-templated silver nanocluster and its application for ratiometric fluorescence target detection with exponential signal response [J]. *Advanced Functional Materials*. 2017; 27(46):1704092.
75. Fu Y, Zhang J, Chen X, et al. Silver nanomaterials regulated by structural competition of G-/C-Rich oligonucleotides [J]. *Journal of Physical Chemistry C*. 2011;115(21):10370-10379.
76. Li T, Zhang L, Ai J, et al. Ion-tuned DNA/Ag fluorescent nanoclusters as versatile logic device [J]. *ACS Nano*. 2011;5(8):6334-6338.
77. Tao G, Chen Y, Lin R, et al. How G-quadruplex topology and loop sequences affect optical properties of DNA-templated silver nanoclusters [J]. *Nano Research*. 2018;11(4):2237-2247.
78. Cui Q, Ma K, Shao Y, et al. Gap site-specific rapid formation of fluorescent silver nanoclusters for label-free DNA nucleobase recognition [J]. *Analytica Chimica Acta*. 2012;724:86-91.
79. Lhara T, Ishii T, Araki N, et al. Silver ion unusually stabilizes the structure of a parallel-motif DNA triplex [J]. *Journal of the American Chemical Society*. 2009;131(11): 3826-3827.
80. Li J, Jia X, Li D, et al. Stem-directed growth of highly fluorescent silver nanoclusters for versatile logic devices [J]. *Nanoscale*. 2013;5(13):6131-6138.
81. Fumiao Shen A, et al. Three-way junction-promoted recycling amplification for sensitive DNA detection using highly bright DNA-silver nanocluster as label-free output [J]. *Talanta*. 2020;206(C):120216-120216.
82. Xiaoxiao Hou. Preparation and Application of DNA Template-guided AgNCs [D]; 2018.
83. Ono A, Cao S, Togashi H, et al. Specific interactions between silver (I) ions and cytosine-cytosine pairs in DNA duplexes [J]. *Chem Commun (Camb)*. 2008;39(39): 4825-4827.
84. Sengupta B, Springer K, Buckman JG, et al. DNA templates for fluorescent silver clusters and i-motif folding [J]. *The Journal of Physical Chemistry C*. 2015;113(45): 19518-19524.
85. Fu Y, Zhang J, Chen X, et al. Silver nanomaterials regulated by structural competition of G-/C-rich oligonucleotides [J]. *Journal of the American Chemical Society*. 2011;115(31):10370-10379.
86. Zhang P, Liu H, Li X, et al. A label-free fluorescent direct detection of live *Salmonella typhimurium* using cascade triple trigger sequences-regenerated strand displacement amplification and hairpin template-generated-scaffolded

- silver nanoclusters [J]. *Biosensors and Bioelectronics*. 2017;87:1044-1049.
87. Chen J, Zhang X, Cai S, et al. A fluorescent aptasensor based on DNA-scaffolded silver-nanocluster for ochratoxin a detection[J]. *Biosensors & Bioelectronics*, 2014, 57: 226-231.
88. Chen C, Shi J, Guo Y, et al. A novel aptasensor for malathion blood samples detection based on DNA-silver nanocluster [J]. *Analytical Methods*. 2018;10(16):1928-1934.
89. Zhou Z, Du Y, Dong S. DNA-Ag nanoclusters as fluorescence probe for turn-on aptamer sensor of small molecules [J]. *Biosensors and Bioelectronics*. 2011; 28(1):33-37.
90. Mills, Dawn M, Foguel, Marcos V, Martin, Christopher P, et al. Rapid detection of different DNA analytes using a single electrochemical sensor [J]. *Sensors and Actuators*. 2019;B293(AUG.):11-15.
91. Yue, Huang Ji, et al. Sensitive detection of chloramphenicol based on Ag-DNAzyme-mediated signal amplification modulated by DNA/metal ion interaction [J]. *Biosensors and Bioelectronics*; 2018.
92. A structure-switchable aptasensor for aflatoxin B1 detection based on assembly of an aptamer/split DNAzyme [J]. *Analytica Chimica Acta*. 2015;886:182-187.
93. Jingwen A Li, et al. Label-free exonuclease I-assisted signal amplification colorimetric sensor for highly sensitive detection of kanamycin – Science Direct [J]. *Food Chemistry*;2021.
94. Cheng R, Liu S, Shi H, et al. A highly sensitive and selective aptamer-based colorimetric sensor for the rapid detection of PCB 77 [J]. *Journal of Hazardous Materials*. 2017;373.
95. Miao M, Tian J, Luo Y, et al. Terminal deoxynucleotidyl transferase-induced DNAzyme nanowire sensor for colorimetric detection of lipopolysaccharides [J]. *Sensors and Actuators B Chemical*. 2017;256.
96. Tao X, He F, Liu X, et al. Detection of chloramphenicol with an aptamer-based colorimetric assay: critical evaluation of specific and unspecific binding of analyte molecules [J]. *Microchimica Acta*. 2020; 187(12).
97. A, Chia Chen Chang, et al. Aptamer-based colorimetric detection of platelet-derived growth factor using unmodified gold nanoparticles [J]. *Biosensors and Bioelectronics*. 2013;42(1):119-123.
98. Tomita Y, Morita Y, Suga H, et al. DNA module platform for developing colorimetric aptamer sensors [J]. *Biotechniques*. 2016;60(6):285.
99. Wang L, Liu X, Hu X, et al. Unmodified gold nanoparticles as a colorimetric probe for potassium DNA aptamers [J]. *Chemical Communications*. 2006(36):3780-3782.
100. Walker GT, Fraiser MS, Schram JL, et al. Strand displacement amplification-an isothermal, in vitro DNA amplification technique [J]. *Nucleic Acids Research*. 1992;20(7):1691-1696.
101. Wang T, Zhang Z, Li Y Y, et al. Amplified electrochemical detection of mecA gene in methicillin-resistant staphylococcus aureus based on target recycling amplification and isothermal strand-displacement polymerization reaction [J]. *Sensors and Actuators B: Chemical*. 2015;221:148-154.
102. Chen A, Gui G F, Zhuo Y, et al. Signal-off electrochemiluminescence biosensor based on Phi29 DNA polymerase mediated strand displacement amplification for microRNA detection [J]. *Analytical Chemistry*. 2015;87(12):6328-6334.
103. Dirks RM, Pierce NA. Triggered amplification by hybridization chain reaction [J]. *Proceedings of the National Academy of Sciences of the United States of America*. 2004;101(43):15275-15278.
104. Zhang B, Liu BQ, Tang DP, et al. DNA-based hybridization chain reaction for amplified bioelectronic signal and ultrasensitive detection of proteins [J]. *Analytical Chemistry*. 2012;84(12):5392-5399.
105. Huang JH, Gao X, Jia JJ, et al. Graphene oxide-based amplified fluorescent biosensor for Hg<sup>2+</sup> detection through hybridization chain reactions [J]. *Analytical Chemistry*. 2014;86(6):3209.
106. Wang R, Wang L, Xu X W, et al. An enzyme-free and label-free fluorescence biosensor for microRNA detection based on cascade amplification of DNAzyme-powered three-dimensional DNA walker and hybridization chain reaction [J]. *Sensors and Actuators B: Chemical*. 2018;268:287-292.
107. Yin P, Choi HMT, Calvert CR, et al. Programming biomolecular self-assembly pathways [J]. *Nature*. 2008;451(7176):318-322.

108. Tao F, Fang J, Guo YC, et al. A target-triggered biosensing platform for detection of HBV DNA based on DNA walker and CHA [J]. *Analytical Biochemistry*. 2018;554: 16-22.
109. Liu HY, Tian T, Zhang YH, et al. Sensitive and rapid detection of microRNAs using hairpin probes- mediated exponential isothermal amplification [J]. *Biosensors and Bioelectronics*. 2017;89:710-714.

---

© 2021 Li et al.; This is an Open Access article distributed under the terms of the Creative Commons Attribution License (<http://creativecommons.org/licenses/by/4.0>), which permits unrestricted use, distribution, and reproduction in any medium, provided the original work is properly cited.

*Peer-review history:*  
*The peer review history for this paper can be accessed here:*  
<http://www.sdiarticle4.com/review-history/66371>